GROWTH CHARACTERISATION OF FATIGUE CRACKS REPAIRED WITH ADHESIVELY BONDED BORON/EPOXY PATCHES

Dr Alan Baker Airframes and Engines Division,
Defence Science and Technology Organisation, Aeronautical and Maritime Research Laboratory, Australia.

ABSTRACT

This study is aimed at characterising crack growth in patched panels under constant amplitude loading. The variables evaluated are: a) patch disbond size, b) applied stress, c) patch thickness, d) ***R*** ratio and e) temperature. For use with the model a simple Paris-type crack growth relationship is assumed between ***da/dN*** and ΔK for the patched crack. The patching system studied consists of pre-cracked 2024 T3 aluminium test panels (~3 mm thick) repaired with boron/epoxy patches, bonded with adhesive FM 73.

Generally, Rose's model for estimation of ΔK in patching situations appears capable of predicting crack growth behaviour for this simple patching configuration quite well, but several issues remain to be resolved regarding the effect of ***R*** ratio and temperature.

KEYWORDS

Aluminium, Aircraft Structures, Fatigue, Repair, Adhesive Bonding, Fibre Composites

1. INTRODUCTION

Crack patching technology (Baker 1988, 1994) - repair of fatigue-cracked components with adhesively bonded advanced fibre composite reinforcements - pioneered in Australia since the mid 1970s has been extensively deployed on RAAF aircraft and more recently on military aircraft in the US and Canada. These repairs have proved to be highly efficient and cost effective. Recently technology was extended to the repair of critical damage in primary structure of the F111 wing skin Baker et al 1996.

Figure 1, based on comparative fatigue tests on edge-notched panels, illustrates the effectiveness of bonded composite repairs compared with mechanical repairs.

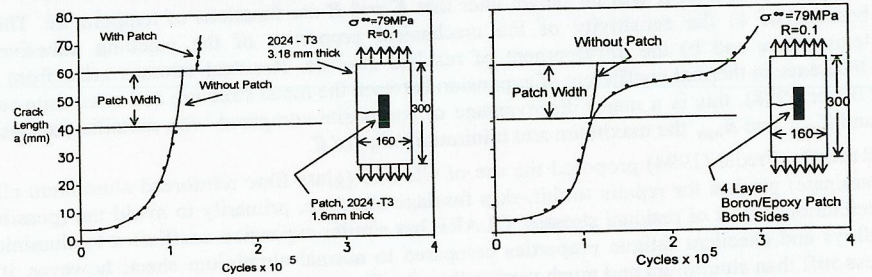

- **Small crack retardation under patch**
- **Rapid growth on exit**
- **Most effective if crack arrests at rivet hole**
- **Cannot detect crack under patch**

- **High crack retardation**
- **Slow growth on exit**
- **Still effective reinforcement**
- **Can monitor crack under patch**
- **Much thinner lighter repair**

Figure 1 *Comparison of crack growth performance of patching efficiency between a mechanically fastened mechanical repair and an adhesively bonded composite repair.*

In Australia the composite generally used for the reinforcement or patch material is boron/epoxy (b/ep) in part because of its high Youngs Modulus (3 × aluminium) and strength, resistance to fatigue, immunity to corrosion and its low electrical conductivity. Low conductivity greatly aids use of eddy-current NDI to detect crack growth under the patch and avoids galvanic corrosion problems which can arises with graphite/epoxy patches. The patches are bonded with an aerospace grade structural epoxy-nitrile film adhesive, usually Cytec® FM 73. Special pre-bonding surface treatments, based on the use of silane coupling agents and primers, were developed to ensure that highly durable bonds can be produced under field repair conditions (Baker and Chester 1992).

2. AIMS OF PROGRAM

The long-term aim is to develop a predictive capability for the growth of patched cracks under spectrum loading. This study is based on an estimate of stress intensity K, using the analytical patching model described in the next section and experimental fatigue studies on a standard patched specimen. Since experimental results are limited at this stage the aim of this paper is essentially to illustrate the approach taken and reach tentative conclusions.

The aim is a) to obtain the crack growth constants under constant amplitude loading and b) to calibrate an appropriate model for load sequence or crack growth retardation effects.

The stress variables under constant amplitude stressing assessed include:

- Stress range: $\Delta\sigma_\infty = \sigma_{max} - \sigma_{min}$ where σ_{min} and σ_{max} are respectively the minimum and maximum stress
- Stress Ratio: $R = \sigma_{min}/\sigma_{max}$

It is assumed that, as for unpatched cracks, a Paris-type relationship $da/dN = f(\Delta K, R) = A_R \Delta K^{n_R}$ holds, where a is crack size, N is number of constant amplitude cycles and A_R and n_R are assumed to constants for a given R. More advanced models based on ΔK effective, taking into account crack closure effects, are not considered at this stage because of complications due to residual stresses.

For patched cracks, it will be shown later that K and R are functions of temperature. This is because of a) the sensitivity of the mechanical properties of the patching adhesive to temperature and b) the development of residual stresses. Residual stresses arise from the difference in thermal coefficient of expansion between the metal structure and composite patch (Baker 1988), this is a major disadvantage of composite compared with metallic patches. R and K_{max} and K_{min} the maximum and minimum value of K.

Recently, Fredel (1994) proposed the use of GLARE (glass fibre reinforced aluminium alloy laminate) patches for repairs to thin-skin fuselage structure, primarily to avoid the (possible) deleterious effect of residual stresses. GLARE has similar expansion coefficient to aluminium alloys and excellent fatigue properties compared to normal aluminium sheet; however, it is less stiff than aluminium and much weaker than the fibre composites.

3. REPAIR DESIGN/ANALYSIS

The aim of the analysis (Baker 1988) is to estimate a) K (and R) as a function of the various geometrical, physical and stress parameters and b) the corresponding stresses in the patch system. Generally, the minimum patch thickness is chosen to obtain the desired stress intensity in the patched crack without exceeding the strength or fatigue strain allowables for the patch system (patch, tensile strain and adhesive, shear strain) to avoid excessive patch stiffness and

to minimise residual stress. The parameters other than applied stress in determining K for a patched panel configuration, as shown in Figure 1b, are:

- Metallic Structure: thickness t_P, ,Youngs modulus E_P, , shear modulus G_P and thermal expansion coefficient α_P
- Patch Reinforcement: thickness t_R, Youngs modulus E_R , and thermal expansion coefficient α_R
- Adhesive: thickness t_A, shear modulus G_A, shear yield stress τ_p under the operating conditions of temperature, humidity and loading rate.
- Disbonds (if any) over the cracked region: length normal to the crack, $2b$.

3.1. *Model for Estimating Patching Efficiency*

In the model developed by Rose (1982) to estimate stress intensity in the patched crack a two-step approach, as illustrated in Figure 2, is used.

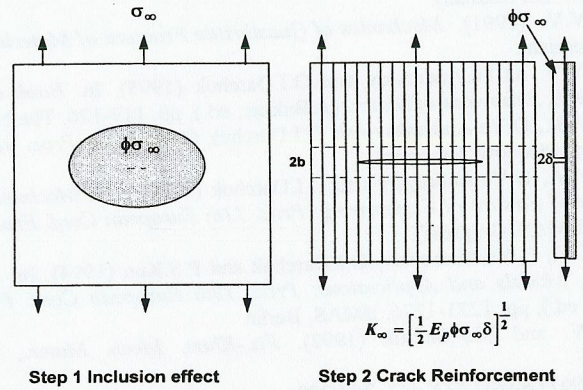

Figure 2: *Schematic illustration of the analytical approach to crack patching. The parallel lines represent a disbond, width 2b.*

In the step 1, Figure 2, the patch is modelled as an inclusion in a large plate; the crack is assumed to be very small compared to the patch. The stress in the metallic component remote from the crack is then given by $\phi\sigma_\infty$, where σ_∞ is the applied stress and ϕ a factor which accounts for the stiffness and shape of the patch. Because the patch attracts load the stress reduction is usually significantly less than predicted simply on the basis of ratio of patch stiffness to plate stiffness.

In the step 2, Figure 2, the region under the patch is modelled; the crack is considered to be semi-infinite in length and is bridged by the patch. The stress intensity K_∞ is then as given by the equation in Figure 2, where δ is the "crack" opening displacement. Since δ is estimated from a overlap joint that would be obtained by cutting a strip through the panel normal to the crack, δ and therefore K_∞ are upper-bound estimates.

Under the cyclic stress range $\Delta\sigma_\infty$ the stress-intensity range ΔK_∞ is given by:

$$\Delta K_\infty = \left[\frac{1}{2} E_p \Phi \Delta\sigma_\infty \Delta\delta\right]^{\frac{1}{2}} \quad (1)$$

Note that the crack length a does not feature in equation 1.

The displacement range $\Delta\delta$ is dependent on the thicknesses and stiffnesses of the patch and of the cracked component and on the thickness, shear modulus and effective shear yield stress of the adhesive. It is important to note that the adhesive properties are highly temperature and strain-rate dependent and will also depend on the level of absorbed moisture. $\Delta\delta$ is also dependent on the residual stress level since this affects the level of external stress at which the adhesive will yield. Calculation of δ is described in reference 1.

Equation 1 is strictly correct only for linear behaviour (no yielding of the adhesive) but provides a good estimate of ΔK_∞ provided shear yielding in the adhesive is limited, say, to less than 0.2.

The assumption that the crack growth behaviour follows the relationship:

$$da/dN = A_R(\Delta K_\infty)^{n_R} \tag{2}$$

leads to the conclusions that da/dN will be independent of a. Thus a should be linearly related to N.

Finally, the relationship between crack length **a** and the number of cycles **N** can be obtained from:

$$a = A_R \int_0^N (\Delta K_\infty)^{n_R} dN \tag{3}$$

3.2. *Extension of the Model for Growth of Disbond Damage in the Patch System*

The above analysis was modified (Baker 1993) to allow for the reduction in patching efficiency with disbond growth in the patch system. It is assumed in this simple extension to Rose's analysis that a parallel disbond, size $2b$, traverses the specimen, as illustrated in Figure 2.

Then the opening of the gap is increased by $2be$, where e is the estimated strain in the reinforcement.

Then equation 1 becomes:

$$\Delta K_\infty = \left[\frac{1}{2} E_p \Phi \Delta\sigma_\infty (\delta + 2be)\right]^{\frac{1}{2}} \tag{4}$$

If it is assumed as a first approximation (based on previous fatigue tests on double-overlap joints,[1] Baker 1988) that db/dN is a constant for given stressing conditions, then:

$$b = N\left(\frac{db}{dN}\right) \tag{5}$$

Thus the effect of disbond growth on crack growth behaviour can be estimated using equation 4. If the disbond size is constant, b remains constant in equation 4.

With disbond growth ΔK_∞ is no longer remains constant but follows a square root relationship as a function of b = f(N). Thus, for expected values of n_R a parabolic relationship between a and N is predicted from equation 3 and 4.

Rose (1987) has developed a more sophisticated treatment of the effect damage growth in the patch system, leading, however, to similar conclusions.

4. FATIGUE STUDIES

5. EXPERIMENTAL PROCEDURE

Fatigue crack propagation tests were conducted on 2024 T3 specimens 3.14 mm thick having starting cracks about 5mm long repaired with unidirectional boron/epoxy (Textron 5521/4) patches (unless otherwise mentioned) 7 plies (0.9 mm) thick. In later studies a layer of FM 73 adhesive was cocured onto the boron/epoxy bonding surface. The patches were then bonded with adhesive FM 73 at 120°C, following surface treatment of the metal using the silane process (Baker and Chester 1992) and the boron/epoxy patches by blasting with alumina grit, either directly onto boron/epoxy (in the early studies) or (in the later studies) onto the cocured adhesive layer.

In the fatigue tests, two similar panels are simultaneously tested, joined together as a honeycomb sandwich panel, Figure 3.

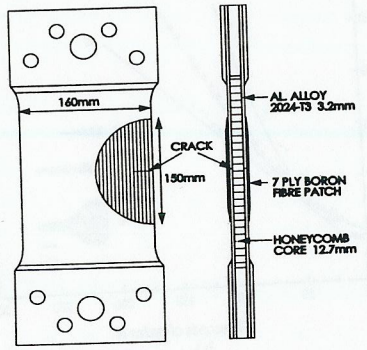

Panel	Patch	Adhesive	Units
E_P = 72	E_R = 200	-	GPa
G_P = 27	G_R = 10	G_A = 0.57, 20°C = 0.25, 60°C = 0.17, 80°C = 0.11, 00°C	GPa
-	-	τ_p = 36, 20°C = 16, 60°C = 12, 80°C = 8, 100°C	MPa
t_p = 3.14	t_R = 0 .52 = 0.90 = 1.30	t_A = 0.4	mm
α_p = 23E-6	α_R = 4E-6	-	$°C^{-1}$

Figure 3: *Test configuration used to evaluate patching efficiency in patched panels. A 7 ply patch is standard but 4 and 10 ply patches were also evaluated. The table provides properties assumed in the calculations based on Cytec short-overlap shear data .*

There are two reasons for using this configuration: The first is to minimise curvature following patching due to the residual stress σ_T which, as mentioned earlier, arises from the mismatch in thermal expansion coefficient between the patch material and the metal panel. Thus, the patches were bonded to the panels at the same time as the panels were bonded to the honeycomb core. The second reason is to minimise the secondary bending of the panels which would otherwise occur during testing. The bending moments arise from the displacement of the neutral plane by the patch. The resistance to bending resulting from the honeycomb core is considered to be a reasonable simulation of the level of support that would be provided by typical military aircraft structure. In almost all tests, similar rates of crack growth were observed for the two panels in the combination.

Tests were conducted under constant amplitude stressing to a maximum of 244MPa at a range of temperatures up to 100°C and applied R values to 0.64. However, a stress of 138MPa and nominal R of 0.1 and ambient temperature was standard.

After testing, the patches were heated to 190°C for 2 hours and stripped from the test specimen (at the elevated temperature). This discolours any disbonded regions by oxidation, making them clearly visible.

6. DISBOND DAMAGE IN THE PATCH SYSTEM

In these studies (Baker 1993, 1994) the aim was to evaluate the effect of disbond growth over the cracked region. The disbonds did not occur in the adhesive but within the surface layer of the boron/epoxy, which consists of a very light scrim of glass cloth, impregnated with the matrix epoxy resin.

A series of specimen were made with artificial disbonds (using thin PTFE sheet inserts) of length 2**b** ranging from 10 mm to 60 mm. Tests were conducted at a peak stress of 138 MPa and R = 0.1. The crack-growth results, Figure 5a, show that, as expected, patching efficiency falls dramatically with increasing disbond size.

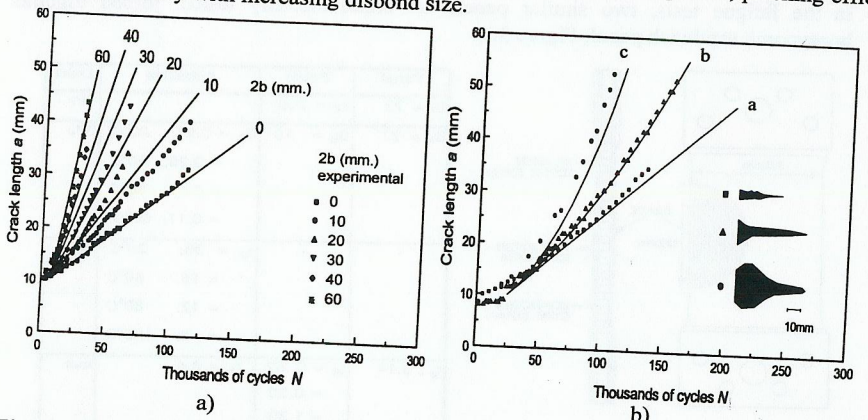

Figure 4: a) *Plot of crack length (**a**) versus cycles (N) for a patched specimen having artificial disbonds of various lengths; solid lines are theoretical estimates, based on estimated A_R and n_R. b) Plot of crack length (**a**) versus cycles (N) for patched panels tested at a peak stress of 138 MPa and nominal **R** = 0.1.*

Figure 4b plots crack length ***a*** versus ***N*** at a peak stress of 138 MPa and ***R*** = 0.1 for three test panels The observed final disbond shapes (2***b***) are shown inset in the figure. As seen in Figure 4, the greater the final disbond size the greater crack growth rate and the more parabolic the curve of ***a*** versus ***N*** ; for a small disbond ***a*** versus ***N*** is linear. These observations are in agreement with predictions of the patching model described in section 3.2.

Figure 4 also shows, as solid curves, labelled a to c, the predicted behaviour based on the foregoing analysis and the final disbond growth rates respectively of 0, 6 $\times 10^{-5}$ and 20×10^{-5} mm/cycle. To produce these curves an Excel spreadsheet was developed to estimate ***da/dN*** and thus ***a*** versus ***N*** based on equations (2), (3), (4) and (5); where A_R and n_R for equation (2) are determined experimentally from patched panels with artificial disbonds. Using the method described in reference 2, this data was used to estimate A_R which was found to be around 5×10^{-11} and n_R around 3.

The estimates for the disbond growth rates, ***db/dN***, for use in equation 5 are obtained from the observed *maximum* disbond size observed in the tests divided by ***N***. Thus the disbond growth

rates assumed in producing the theoretical curves, although an overestimate, are a reasonable approximation.

On the basis of the results provided here (and more fully in reference 2) the tentative conclusion reached is that the model outlined in section 3.2 can account for the influence of disbond growth in the patch system on patching efficiency.

A major input to this model is the relationship between ***db/dN*** and cyclic stress or strain level. This relationship can be obtained empirically from tests on equivalent double-overlap joint specimens representing the repair configuration. However, to estimate ***db/dN*** generically from repair design data, stress patch geometry etc, a suitable damage criterion for the adhesive is required. In the preliminary tests on representative bonded joints (Baker 1988) the effective shear strain range in the adhesive ($\Delta\gamma_A$) was used as the damage criterion, alternative criteria based on energy release rate was used as the damage criterion, alternative criteria based on energy release rate are also under investigation (Baker and Chalkley to be published).

In the current studies briefly described in the following sections the patch was formed with a cocured layer of adhesive. This produces a patch system more resistant to disbond damage, resulting in a change in the locus of the disbond damage from the patch/adhesive interface into cohesive failure in the adhesive.

7. STRESS RANGE

Figure 6a plots the results for ***a*** versus ***N*** for a 7 ply specimen for ***R*** = 0.1 at σ_{max} levels ranging from 80 to 244MPa. The highest stress level corresponds to a limit load capability for this alloy and was thus very close to the level (248MPa) used for the peak stresses in the FALSTAF studies (Raizenne et al 1994). Limit load is nominally experienced only once in the life of an aircraft.

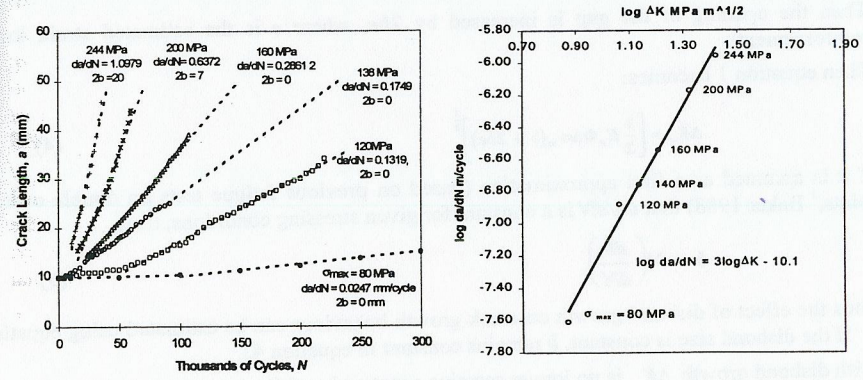

Figure 5: *a) Plots of crack length **a** versus cycles N for a standard 7 ply patched specimen for applied **R** = 0.1. b) Plot of log **da/dN** versus log ΔK_∞ for the results in 5 a).*

The change from a linear relationship to a parabolic relationship occurs above σ_{max} = 138 MPa and results from the development of damage in the adhesive layer, as indicated as a ***2b*** value in the figure. For the standard 138 MPa stress level damage in the adhesive system is negligible, so as expected, patching efficiency is comparable to the best of the previous series, Figure 4.

A linear least squares fit was used to obtain ***da/dN*** for all the stress levels, despite the disbond damage found at the two highest stresses. The high stress values at small crack lengths are included since they fit well with the other results; however, if only the large crack ***da/dN*** values at high stress levels are considered these lie well to the left of the curve, as expected for damage. Using these results, Figure 5 b) plots log ***da/dN*** versus log ΔK_∞ for these test specimens which confirms that the results fit the expected Paris-type relationship. The relationship thus obtained is $da/dN = 7.9 \times 10^{-11} \Delta K_\infty^3$ m/cycle, which is close to the results obtained for the damage series mentioned in the previous section.

8. PATCH THICKNESS

Figure 6 plots log ***da/dN*** versus log ΔK_∞ for test panels with 4, 7 or 10 ply thick patches, at an ***R*** value of 0.1. The results for the 7 ply panel are as plotted in Figure 5 b); the results for the 4 and 10 ply panels were obtained from single test panels stressed at several levels.

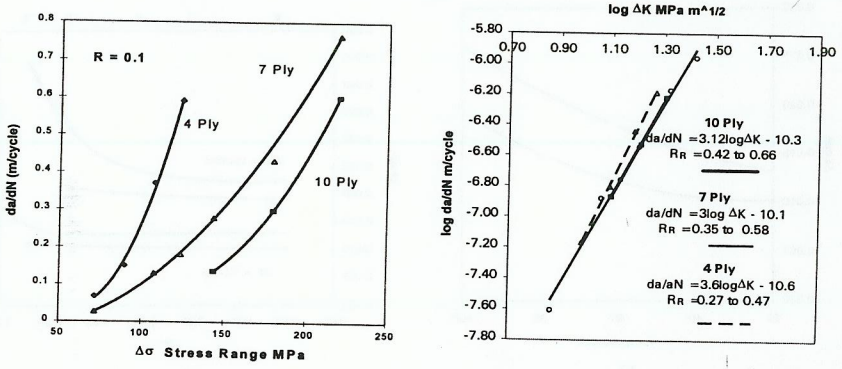

a) b)

Figure 6: *Plots* a) of ***da/dN*** *versus* $\Delta\sigma$ *and b) log* ***da/dN*** *versus log* ΔK_∞ *for test panels having 4, 7 or 10 ply patches.* ***R*** *is 0.1,* R_R *is as indicated on b) and.* t_A *is about 0.5mm.*

It can be seen from Figure 6 that the model using the ***da/dN*** relationship for the 7 ply panel would have given quite reasonable predictions for the 4 and 10 ply panels. However, the values obtained are: 4 Ply: $n_R = 3.6$, $A_R = 2.3 \times 10^{-11}$; 7 ply: $n_R = 3$, $A_R = 7.7 \times 10^{-11}$; 10 ply: $n_R = 3.12$, $A_R = 5 \times 10^{-11}$. While these results appear very promising further experimental results are needed before any firm conclusions can be made.

9. *R* RATIO

For an unpatched specimen $R = \sigma^\infty_{min} / \sigma^\infty_{max}$, whereas for a patched specimen due to residual stress R_R the effective ratio is given by:

$$R_R = (R\phi\sigma_\infty + \sigma_T)/(\phi\sigma_\infty + \sigma_T) \qquad 7$$

where σ_T is the thermal residual stress, which has a maximum value of :

$$\sigma_T = t_R E_R E_P \Delta T(\alpha_P - \alpha_R)/(t_P E_P + t_R E_R) \qquad 8$$

where ΔT = (adhesive cure temperature - operating temperature)

Thus $R_R > R$ and varies with stress level for a constant ***R***. For the standard 7 ply patched panel at σ_{max} = 138 MPa and ***R*** = 0.1, R_R = 0.58.

To evaluate the effect of ***R*** standard 7 ply panel tests were conducted at ***R*** values of 0.1 (standard), 0.4, 0.55 and 0.64 at $\Delta\sigma$ = 72 MPa. Stresses were kept fairly low to avoid adhesive damage which would have complicated the outcome of the tests. Figure 7 shows the results of a) ***a*** versus ***N*** and b) log ***da/dN*** versus log ΔK_∞.

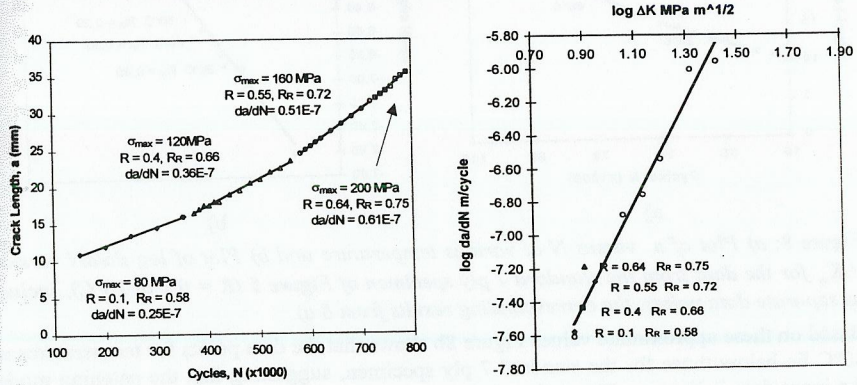

a) b)

Figure 7 a) Plot of ***a*** *versus* ***N*** *for* ***R*** *values as shown for a standard 7 ply test specimen and b) Plot of log* ***da/dN*** *versus log* ΔK_∞ *for the data from the 7 ply specimen (****R****=0.1) of Figure 6b, including, as solid data points the corresponding results for different* ***R*** *ratios from 8 a).*

As seen in Figure 8b, the data points for $R > 0$ fall close to the curve for $R = 0.1$ which is pleasing but unexpected since a higher crack growth rate would be expected at the higher ***R*** level so that these data points should lie to the left of the curve. However, studies (Baker 1994) at low temperatures[2] (-40°C) where R_R is also high, (0.55) showed no observable change in crack growth rate compared to ambient so also suggest an insensitivity to **R**.

10. TEMPERATURE

The influence of temperature on crack propagation behaviour in patched specimens is quite complex (Baker 1993, 1994) since the following changes occur:

- A change in ***R*** since residual stress reduces as temperature increases
- A change in patching efficiency:
  ΔK_∞ is increased as temperature increases because of a decrease in adhesive shear modulus G_A and shear yield stress τ_p,
  ΔK_∞ is increased if the rate of disbond damage increases with increasing temperature
- A change in the crack propagation properties of the alloy itself

To investigate the influence of temperature tests were conducted on a standard 7 ply specimen at a stress level of 138 MPa at 20, 60, 80 and 100°C. Estimations of ΔK_∞ for the log plots against ***da/dN*** were based on the temperature values of G_A and τ_p provided in the table with Figure 3. Figure 8 shows the results of a) ***a*** versus ***N*** and b) log ***da/dN*** versus log ΔK_∞.

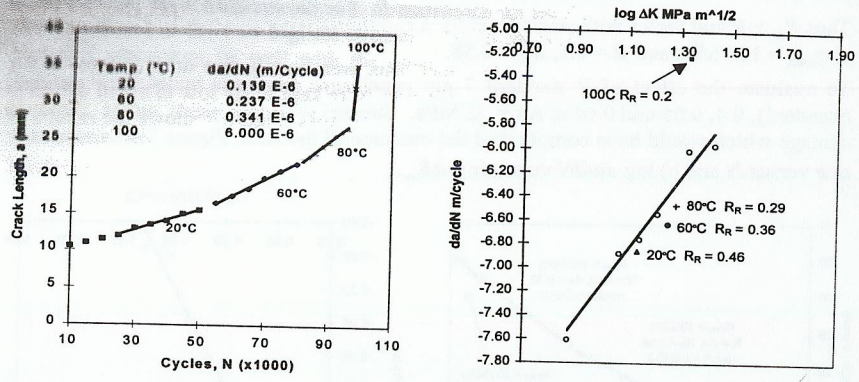

a) b)

Figure 8: *a) Plot of* a *versus* N *at various temperature and b) Plot of log* da/dN *versus log* ΔK_∞ *for the data from the standard 7 ply specimen of Figure 5 (R = 0.1 at 20°C), including, as separate data points, the corresponding results from 8 a).*

Based on these approximate values Figure 8b shows that the data points for temperatures up to 80°C lie below those for the standard 7 ply specimen, suggesting that the patching model or the input data is in error. The main problem using the model is to know what values to take for the adhesive properties at elevated temperature because both temperature and strain rate have to be taken into account; the values used (Table in Figure 3) for G_A and τ_p were based on static measurements and so will be low compared to dynamic values appropriate to the fatigue test conditions.

To investigate more directly the influence of R and temperature studies were conducted on representative bonded joints.

11. STUDIES ON REPRESENTATIVE BONDED REPAIR JOINTS

Studies are being conducted on joints (depicted in Figure 9) representing a section through the cracked/patched region to assess the influence of the variables temperature and R on the "crack opening range" $\Delta\delta$ and to compare these measurements with the theoretical estimates. To avoid complications associated with boron/epoxy patches (including shear lag and residual stresses) these initial tests were made on joints with aluminium outer adherends, of equal stiffness to the inner adherend. Earlier work on this topic is reported by Baker 1988.

Measurement of $\Delta\delta$ provides an assessment of the effective mechanical properties of the adhesive under cyclic loading and provides through equation 1 an experimental estimate of the influence of the patching variables on ΔK_∞ . Note that ΔK_∞ (an upper-bound estimate of ΔK) is proportional $(\Delta\delta)^{1/2}$; thus $[\Delta\delta(\text{experimental})/\Delta\delta(\text{theoretical})]^{1/2}$ provides an estimate of the error in calculating ΔK_∞.

Figure 9a plots the measurements of $\Delta\delta$ over a range of temperatures for an all-aluminium joint (at a cyclic frequency of 3 Hz), and Figure 9b plots $\Delta\delta$ for a range of R ratios. Also shown are the calculated results based on the adhesive mechanical property data provided in the table in Figure 3; formulae used to obtain $\Delta\delta$ are as given by Baker 1988.

Considering firstly temperature, Figure 9a shows that the theoretical estimate of $\Delta\delta$ versus temperature is higher than the experimental value, indicating that the assumed adhesive properties may be too low. Stress levels were kept low in these tests to avoid damage to the adhesive. As there should be little plastic yielding of the adhesive at the low stress levels used, the main temperature-dependent variable influencing $\Delta\delta$ is the shear modulus G_A. To obtain agreement between the theoretical and experimental results a factor of about two on the G_A assumed is required. This is not unexpected since the mechanical properties used were based on a rate of loading significantly lower than the 3 Hz used in these tests. At higher stress levels, where yielding occurs, a significant underestimate is also expected in the shear yield stress τ_p. Thus use of higher G_A and τ_p values is justified and could explain the temperature results, Figure 8.

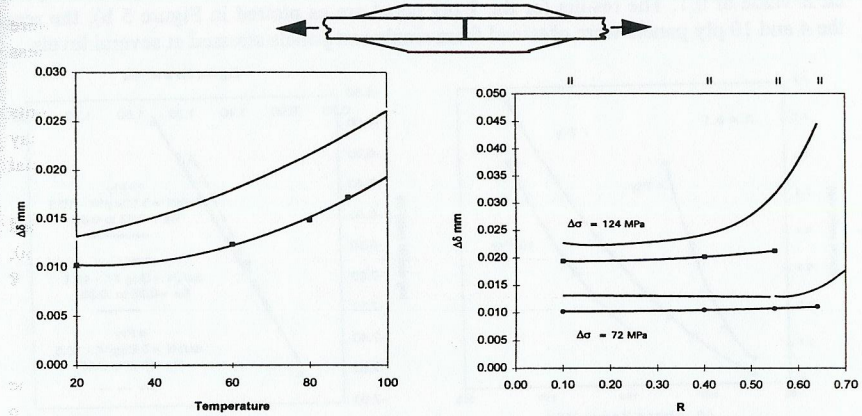

a) b)

Figure 9: *Plots of* $\Delta\delta$ *for an all-aluminium double overlap joint shown above, versus a) temperature for* $\Delta\sigma = 72$ and $R = 0.1$ *and b)* R *for the stress conditions indicated. The upper line in each set is the theoretical estimate; the break in the curve at the lower stress level is due to the transition from the use of all-elastic to elastic/plastic equations.*

Considering experimental results for $\Delta\delta$ versus R, Figure 9b shows that the relationship is very flat. This result suggests an insensitivity to R in fatigue crack propagation of patched cracks - in accord with the observed behaviour, Figure 7. However, in this all-aluminium joint $R_R = R$, which significantly lower than for a similar joint with boron/epoxy outer adherends.

The predicted curves of $\Delta\delta$ versus R is also fairly flat at low R values, in agreement with experiment; however, the predicted curve is higher than the experimental curve indicating again possible error in assuming the static stress/strain rather than dynamic properties for the adhesive. At high R and particularly at high stress levels where significant yielding of the adhesive occurs the predicted $\Delta\delta$ versus R relationship becomes much stronger. The predicted curve for the representative bonded joint with the boron/epoxy outer adherends shows this effect at lower R values, but this behaviour has yet to be confirmed experimentally.

12. CONCLUSIONS

Studies were made on the constant-amplitude crack growth behaviour on cracked 2024 T3 aluminium panels (~3 thick) having boron/epoxy patches bonded with adhesive FM 73 to

validate Rose's crack-patching model. The variables evaluated were: a) patch disbond damage b) applied stress, c) patch thickness, d) R ratio and e) temperature. Although more data is required to reach a firm conclusion, tentative findings are as follows:

1. **Patch Disbond Damage**: A simple modification was made to the model to allow for disbond growth. The (modified) model predicts the correct form of the a versus N crack growth relationship for disbond growth in the patch system - linear for little disbond growth changing to parabolic for significant growth and, based on few results, produces reasonable quantitative predictions.
2. **Applied Stress**: Using the model (no disbond damage) to estimate ΔK (for a 7 ply boron/epoxy patch, R = 0.1) a straight line relationship was obtained between log da/dN and log ΔK having A and n constants of the correct order for aluminium alloy 2024 T3.
3. **Patch Thickness**: The log da/dN and log ΔK relationship for 4, 7 and 10 ply patches were similar suggesting that the model can give satisfactory predictions for patch stiffness variations over this range.
4. **R ratio**: The results indicate an insensitivity to R for values from 0.1 to 0.64, since points (for 7 ply patches) at high R fall on the log da/dN and log ΔK curve for R = 0.1. This may be a feature of patched cracks since low-temperature results (-40°C) where due to residual stresses R is very high have no observable effect on da/dN.
5. **Temperature**: On the basis of the log da/dN and log ΔK relationship for the 7 ply patched panels at 20°C, the model appears to overcompensate somewhat for temperatures of 60, 80°C. Based on the representative bonded joint the problem for both the temperature and R predictions may be the assumption of too low adhesive properties.

13. ACKNOWLEDGEMENTS

The Author would like to thank Onofrio Beninati and Paul Chapman for conducting the experimental work and Drs Francis Rose, Richard Chester and Chun Wang for comments on the manuscript.

14. REFERENCES

Baker A.A., Crack Patching: "Experimental Studies, Practical Applications", Chapter 6. in *Bonded Repair of Aircraft Structures*, Editors Baker A.A and Jones R, Martinus Nijhoff, 107-173 1988. Chapter 6.

Baker A.A. and Chester R.J., "Minimum Surface Treatments For Adhesively Bonded Repairs" *International Journal of Adhesives and Adhesion* **12** (1992), pp. 73-78.

Baker A.A., "Bonded Composite Repair of Metallic Aircraft Components", Paper 1 in AGARD-CP-550 Composite Repair of Military Aircraft Structures, 1994.

Baker A.A., "Repair Efficiency in Fatigue-Cracked Panels Reinforced with Boron/Epoxy Patches" *Fatigue and Fracture of Engineering Materials and Structures* **16** (1993), pp. 753 - 765.

Baker AA, Rose L.R.F, Walker K.F. and Wilson E.S.,"Repair Substantiation for a Bonded Composite Repair to a F-111 Lower Wing Skin" Proceedings of the Air Force 4th Aging Aircraft Conference, Colorado July 1996.

Chalkley P. and Chiu W.K., "An Improved Method for Testing the Shear Stress/Shear Strain Behaviour of Adhesives" *International Journal on Adhesion and Adhesives* **13** (1993). pp. 237-242.

Davis M., "The Development of an Engineering Standard for Composite Repairs," Paper 24 in AGARD-CP-550 Composite Repair of Military Aircraft Structures, 1994.

Fredell R.S., van Barnveld W. and Vlot A., "Analysis of Composite Crack Patching of Fuselage Structures: High Patch Modulus Isn't the Whole Story", SAMPE International Symposium 39, April 1994.

Rose L.R.F., "A Cracked Plate Repaired by Bonded Reinforcements" *International Journal of Fracture* **18** (1982) pp. 135 - 144.

Rose L.R.F, "Influence of Disbonding on the Efficiency of Crack Patching", *Theoretical Applied Fracture Mechanics* 7 (1987) 125-132.